d/p and t/p ratios in nucleon-nucleus and heavy ion reactions: Can entropy be determined?

A. Fokin,[1] L. Carlén,[1] R. Ghetti,[1] B. Jakobsson,[1] J. Mårtensson,[1] Yu. Murin,[1] A. Oskarsson,[1] C. Ekström,[2] G. Ericsson,[2] J. Romanski,[2] E. J. van Veldhuizen,[2] L. Westerberg,[2] K. Nybö,[3] T. F. Thorsteinsen,[3] S. Amirelmi,[3] M. Guttormsen,[4] G. Løvhøiden,[4] V. Bellini,[5] F. Palazzolo,[5] M. L. Sperduto,[5] J. P. Bondorf,[6] I. Mishustin,[6] V. Avdeichikov,[7] O. V. Lozhkin,[8] W. A. Friedman,[9] and K. K. Gudima[10]

(CHIC Collaboration)

[1]*Department of Physics, University of Lund, Lund, Sweden*
[2]*The Svedberg Laboratory, University of Uppsala, Uppsala, Sweden*
and Department of Neutron Physics, University of Uppsala, Uppsala, Sweden
[3]*Department of Physics, University of Bergen, Bergen, Norway*
[4]*Department of Physics, University of Oslo, Oslo, Norway*
[5]*INFN/LNS, University of Catania, Catania, Italy*
[6]*Niels Bohr Institute, Copenhagen, Denmark*
[7]*Joint Institute for Nuclear Research, Dubna, Russia*
[8]*V. G. Khlopin Radium Institute, St. Petersburg, Russia*
[9]*Department of Physics, University of Wisconsin, Madison, Wisconsin 53706*
[10]*Institute of Applied Physics, Kishinev, Moldavia*

(Received 3 December 1998; published 25 June 1999)

The relative yields of high energy deuterons and tritons as compared to protons have been measured in $p+\mathrm{Kr}$, $^{16}\mathrm{O}+\mathrm{Kr}$ and $^{20}\mathrm{Ne}+\mathrm{Ar}$ reactions with a continuously varying beam energy up to $500A$ ($400A$) MeV. Statistical (expanding) evaporation models are not able to reproduce these d/p or t/p ratios, which for high particle energy (>30 MeV) increase smoothly with beam energy. Models that contain nucleon-nucleon scattering, like cascade or nuclear molecular dynamics models, can only reproduce the ratios if a final-state interaction is introduced via the coalescence prescription. The coalescence radius that best fit the data is rather constant over wide beam energy intervals. Entropy can, however, not be directly determined from these ratios. [S0556-2813(99)05607-1]

PACS number(s): 25.70.Mn, 25.70.Pq

I. INTRODUCTION

Attempts to estimate entropy [1] of the participant zone by means of fragment yield ratios have been made. It was suggested that the entropy (S) of a finite size (mass, A) nucleus excited to (ϵ^*) less than a few tens of MeV/nucleon can be determined from the ratio (R_{xN}) between the yield of a composite particle (x) and a nucleon [2]. A simple formula which relates S/A to the density of nucleons, ρ_N, and thus to R_{dp} for an expanding Fermi-Dirac system in chemical equilibrium is

$$S/A = 5/2 - \ln(2^{2/3}\langle\rho_N\rangle) = 3.95 - \ln(R_{dp}), \qquad (1)$$

provided that the number of protons is much larger than the number of deuterons and that heavier clusters can be neglected. Data for heavy ion collisions at $400A$ MeV [1], used in Eq. (1), seem to vastly overestimate the entropy. The necessity to introduce additional degrees of freedom, like isospin excitations (pion production), has been discussed [3] but for energies discussed in this paper this cannot explain the large entropy determined from the d/p or t/p ratios. On the other hand, complete calculations, based on either hydrodynamical models [4] or statistical models [5], have been introduced to determine the entropy. There it was shown that secondary decay plays an essential role for the S/A-R_{dp} relation whereas the breakup density plays a lesser role when kept within reasonable limits, say $\rho/\rho_0 = 0.3-1.0$. More recently also the prescription of expanding systems that sequentially evaporate and/or rapidly decay (multifragmentation) has been discussed in terms of the S/A-R_{xp} relation [6]. Such calculations, as well as pure evaporation calculations, microscopic [7,8], and mean-field calculations that contain nucleon-nucleon (NN) scattering, have been confronted with our data. In the NN calculations multinucleon clusters are produced in final-state interactions through the coalescence prescription and we discuss in this paper how to interpret the results when comparing to the d/p and t/p data.

In the early data [1,9,10] from asymmetric (light-projectile–heavy-target) reactions at $16A$ MeV to $1A$ GeV it appeared as if an evaporative liquid-drop formalism with an assumption about global thermal equilibrium better describes the combined information from d/p, t/p, and α/p ratios than a free strongly interacting gas prescription [11]. This may be a natural consequence of the fact that low energy, light particle production is dominated by evaporation from a weakly excited targetlike source. In this paper we select instead particles from the strongly interactive, highly excited part of the collisions by proper cuts in momentum space. These data are compared to R_{dp} ratios from $p+\mathrm{Kr}$

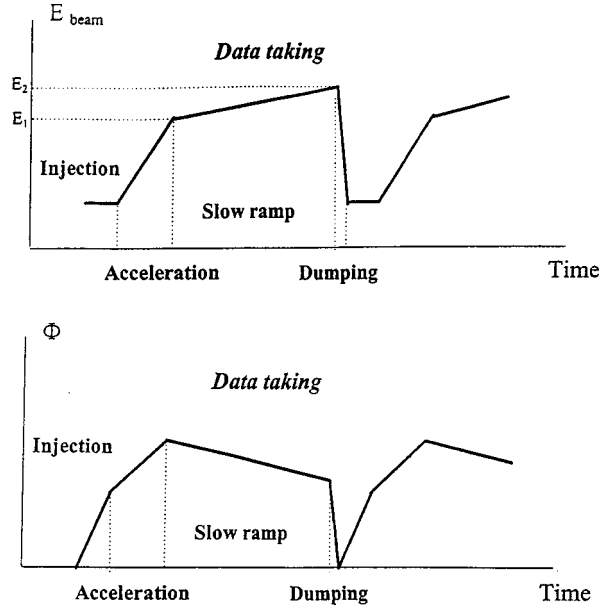

FIG. 1. Schematic representation of the beam energy and flux variation with time during one cycle of stored beam particles.

collisions at beam energies up to 500 MeV which, however, correspond to substantially lower excitation energies, only up to 6*A* MeV.

II. EXPERIMENTAL DETAILS

All experimental data, presented in this paper, were collected at the CELSIUS storage ring, which can provide beams of protons up to 1360 MeV and $Z/A=1/2$ heavy ions up to 470*A* MeV with luminosities L up to 1×10^{31} cm^{-2} s^{-1} and 1×10^{28} cm^{-2} s^{-1}, respectively. Here $L=\nu\Phi d_t$, where ν is the frequency of the circulating beam, Φ is the number of stored ions, and d_t is the effective target thickness, i.e., the actual thickness that the beam passes through. In our experiments protons and fully stripped ^{16}O and ^{20}Ne ions were injected, rapidly accelerated up to the start energy (E_1), and then stored with the gas jet target in operation while the magnets are slowly ramped [12] until the final energy (E_2) was reached and then finally the beam was dumped. The flux increases during injection due to the increase of the frequency but decreases during the slow ramp since the losses there are larger than the frequency increase. No more than a factor of 3 decrease in Φ is accepted. Figure 1 gives a schematic picture of the energy and flux variation during the cycles with lifetimes varying from 1 to 5 min.

The data presented in this work on *p*, *d*, and *t* were collected in parallel with data on charged pions [12], using the same sandwich, plastic scintillator, range telescopes whenever on-line proton rejection was not necessary for the pion registering. The ten-element telescopes [13] contain NE102 scintillators with successively increasing thickness from 5 mm to 30 mm. The detectors are coupled with Plexiglas light guides to either Hamamatsu R1166 (20° telescope) or Philips XP2020 (all other telescopes) PM tubes. These telescopes were mounted outside thin windows in angular positions from 20° to 150° (Table I) and cover solid angles from 2.5 msr (20°) to 20 msr (150°). There is a 10–20 cm distance between the first three detectors to give direction sensitivity while all other detectors are placed densely together. The trigger requirement is a signal above discriminator in the first two scintillators. The stop detector is defined through a pattern unit controlled off line by the chain of analog-to-digital converter (ADC) signals. Each stop detector produces a ΔE-E correlation with good separation between π, *p*, *d*, and *t* particles. Since only results on d/p and t/p ratios are included in this paper, it should be pointed out that variations in the luminosity are not important and no absolute normalization is necessary. Because of the trigger requirement and of the total telescope thickness of ~20 cm we register ~20–175 MeV protons. Some differences in the energy intervals appear because of the different detector thicknesses in the small volume forward telescopes and the large volume backward telescopes.

TABLE I. List of reactions and detector positions. Data at positions marked with brackets are not further exploited due to small statistics.

Reaction	Angular position	Beam energy
p+Kr	90°	150–500 MeV
O+Kr	(20°) 55°, 75°, 90°, (150°)	22*A*–300*A* MeV
Ne+Ar	(20°) 55°, 75°, 90°, 120°	50*A*–400*A* MeV

III. THEORETICAL CALCULATIONS

A. Models

The momentum space covered in the experiments corresponds to emission almost exclusively from preequilibrium processes, i.e., knockout or pickup processes or early emission from hot strongly interacting regions. Hot and dense regions are chiefly produced in nucleus-nucleus reactions. Any standard three-source prescription confirms that the positions of the particle telescopes exploit the relevant momentum-space regions of preequilibrium particles (Fig. 2). The simulations are in this case based on the nuclear molecular dynamics (NMD) model [14]

It should be noted that the impact parameter (b) is randomly selected with weight ~b in accordance with the inclusive measurements. The left hand side of Fig. 2 shows the situation in p+Kr reactions. At both energies, beamlike protons and protons evaporated from the target source are well separated and not contributing very much to the selected sample. In heavy ion reactions (O+Kr, right hand side) projectile-associated protons are clearly separated from targetlike protons and the intermediate source protons can be identified quite well at 300*A* MeV but not at 50*A* MeV. The heavy ion data we present in this paper start from 100*A* MeV where the preequilibrium source is reasonably well defined. Simulations of *d* and *t* emission within the same prescription show the same general emission characteristics.

The emission of light particles by evaporation from an expanding source is introduced through the model of Fried-

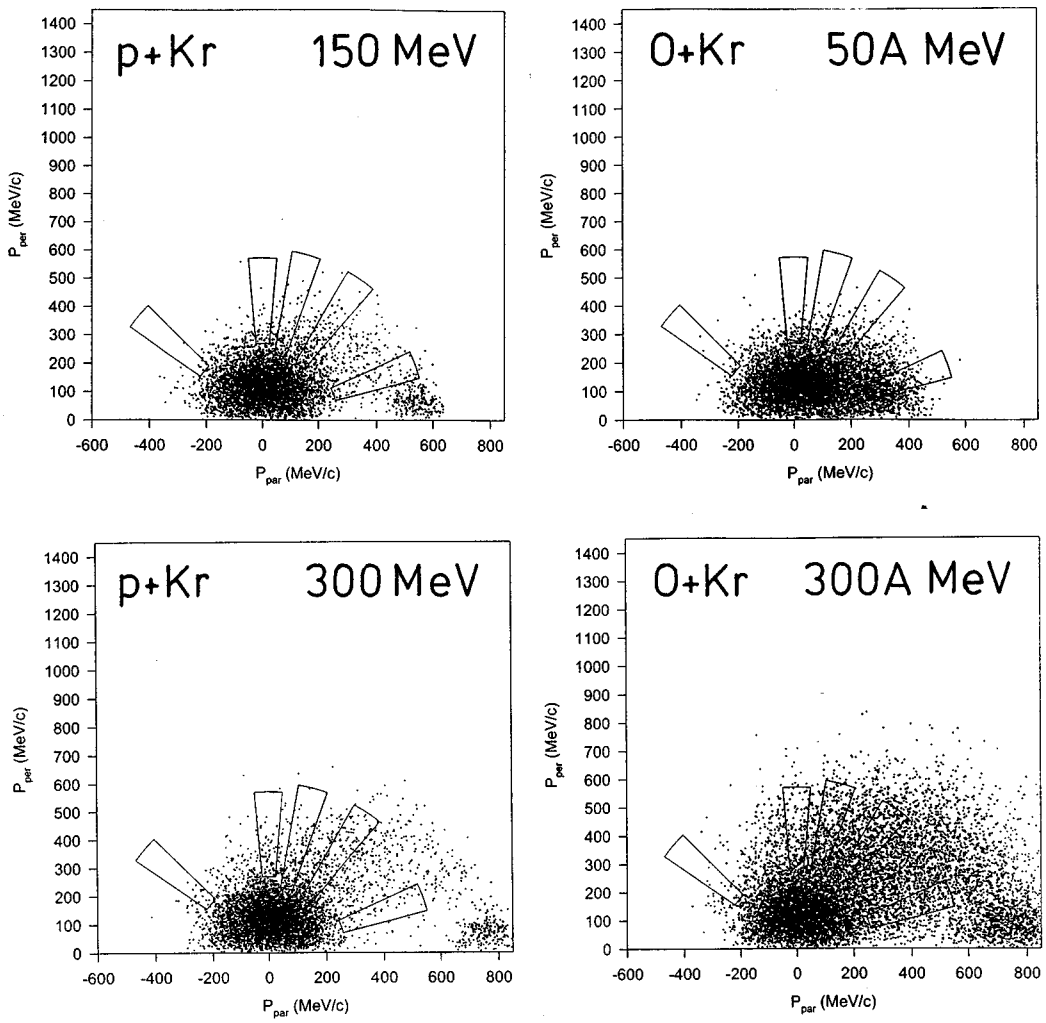

FIG. 2. NMD simulations of proton emission in various reactions and examples of the total momentum-space regions covered by the telescopes.

man [6]. The emission is here treated as a chain of sequential, binary decay processes where the relative decay rates are calculated by detailed balance as proposed in the original Weisskopf prescription for evaporation [15]. These rates are influenced by the conditions associated with the expansion process. In addition secondary contributions of light particles from the decay of unstable resonances are also included. By comparing the sequential calculations to similar calculations within a microcanonical (freeze-out) approach it has been possible to define an effective volume which increases with time during the expansion and allows to estimate a time-dependent entropy of the emitting system.

In addition, ''reference'' calculations within a classical evaporation model, the SIMON code [16], were performed. In this case the time dependence of the entropy is neglected and complete excitation is immediately introduced. This model contains however a more detailed sidefeeding prescription for the secondary decay of primary fragments that are particle instable or excited enough to decay by particle emission.

Microscopic model calculations are represented by the Dubna version of the intranuclear cascade model [7,8]. In this model inelastic nucleus-nucleus interactions are treated as successive quasifree two-particle collisions described by a set of coupled relativistic kinetic equations of Boltzmann type. The description of the mean-field evolution is simplified in the sense that the scalar nuclear potential, defined by the local Thomas-Fermi approximation, remains the same throughout the collision while the potential well depth is changed according to the number of knocked-out nucleons [8]. This procedure allows us to take into account nuclear binding and Pauli blocking. This simplified prescription is relevant for hadron-nucleus and peripheral nucleus-nucleus collisions where no large disturbance on the mean field is expected but it is questionable for violent, central heavy ion collisions.

After completing the cascade stage of the reaction, light particles may be emitted both from equilibrium and nonequilibrium states of excited residual nuclei at a subsequent, more slow stage of the interaction. Preequilibrium emission is here taken into account within the exciton model [17].

We also performed mean-field calculations for the case of d/p in Ne+Ar collisions within the NMD model [14] and we will return to these results in Sec. IV B.

B. Coalescence

In any independent particle model final-state interactions for creating deuterons may be prescribed via the coalescence process. In this prescription, the deuteron cross section is given by the product of the square of the nucleon cross section and the probability to find a proton and a neutron close enough in momentum space,

$$\frac{d^3\sigma_d}{dp^3} = \left(\frac{4\pi}{3}\frac{\gamma p_0^3}{\sigma_r}\right)\left(\frac{d^3\sigma_N}{dp^3}\right)^2 \tag{2}$$

where γ is the Lorenz factor of the beam. The coalescence radius p_0 is either predefined as an effective interaction range, varying from 90 to 115 MeV/c for protons to alpha particles, or empirically determined from d/p^2 radii to be larger, $\sim$190 MeV/c. In more elaborate calculation, $(d^3\sigma_N/dp^3)^2$ must be replaced by $(d^3\sigma_p/dp^3)(d^3\sigma_n/dp^3)$ and the proper n/p ratio of the emitting system should also be introduced. The coalescence prescription has had some success in explaining composite particle emission data.

In cascade models direct use of the coalescence formula at the proper freeze-out time has been introduced [8]. In the NMD model these particles are produced directly, if nucleons are close enough in configuration space. Very few deuterons and tritons can, however, be produced this way and therefore coalescence is introduced as a final-state interaction. In the next section we will return to this formalism when comparing data to calculations.

IV. EXPERIMENTAL RESULTS

A. Proton-nucleus collisions

Figure 3 shows the measured d/p ratio (histograms) for high energy particle emission at 90° in the $p+$Kr reaction from 150 MeV to 500 MeV. Typical statistical errors are presented on a few points only in this figure and in the forthcoming ones. The lower histogram contains protons and deuterons in the same velocity or energy/nucleon bin and their position in the $p_\parallel$-$p_\perp$ plane (Fig. 2) could therefore easily be identified ($p \geqslant 240$ MeV/c). The upper histogram represents particles with the same total kinetic energy (E) which is more natural when comparing to expected Maxwellian sources, $\sim\sqrt{E}\exp(-E/T)$.

In order to determine the entropy from Eq. (1) the total yield from the source is required. This is not possible from these data, but if the 90° emission is representative, the S/A values decrase from 6.5 to 6 when the high energy cut is made and from 9 to 7 for the high energy/nucleon cut. This confirms the strong overestimation of entropy when determined this way.

In both samples the d/p ratio increases monotonically. This is very much the result of the particle energy cuts. Actually, experimental ratios for total yields in heavy ion reactions have shown little dependence at slightly lower beam velocities [18] and some decrease at slightly higher beam energies [2] which follow the expected increase of entropy with increasing beam energy. The cascade approach presents however the increase of the d/p ratios in our data quite properly if deuteron production from final-state coalescence is accepted. In order to describe the very high energy production of deuterons introduced through the energy per nucleon cut, the coalescence radius in momentum space (p_0) must be given a somewhat larger value than 90 MeV/c, which was originally introduced from comparison with heavy ion collision data [1,8]. The proper value for $p+$Kr seems to be 110–120 MeV/c and it does not seem to depend on the beam energy at all in the interval 150–500 MeV. If we include also lower energy deuterons (upper histogram), some target evaporation will certainly be included and it appears rather as if a lower p_0 must be introduced in this case. It should, however, be stressed that an additional introduction of a ''convergence'' criterion, i.e., that the relative velocity $\overrightarrow{v_{ij}}$ is ''attractive'' in the definition of a coalescence cluster, also gives the proper reduction of the d/p level as shown by the dashed curve. If this criterion is to be introduced for the high velocity cut, one should, however, expect an even larger p_0, 130–140 MeV/c.

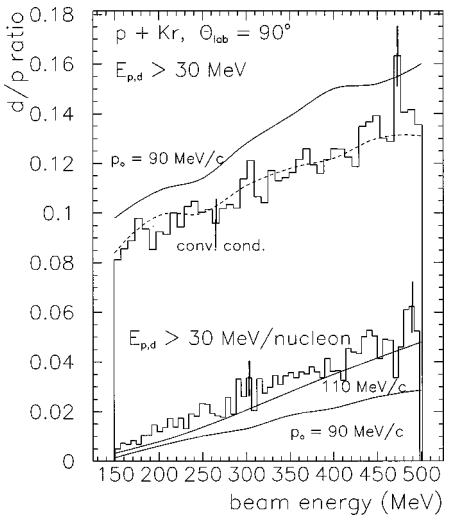

FIG. 3. High energy d/p ratio in $p+$Kr collisions. The upper histogram shows the data for the high energy and the lower for the high energy per nucleon cut. The uppermost and lowermost curves are the results of a cascade calculation [7] including coalescence with a cluster radius of 90 MeV/c and the upper solid curve in the lower part with a radius of 110 MeV/c, while the dashed curve represents cascade calculations with an additional cluster convergence condition (see text).

The fact that high energy particles that were selected must come from early emission processes is further stressed by the ''reference'' NMD calculations. Without introducing coalescence, the d/p ratio falls much below the data, but after its introduction, somewhat arbitrarily at $>$200 fm/c, it is possible to obtain good agreement with the experimental data over the whole beam energy region also in the NMD prescription.

A comparison to pure statistical models, like the EES model, requires that the emission source be predefined. For $p+$Kr collisions the obvious first choice of such a source in thermal and chemical equilibrium would be a compound nucleus with excitation energy 2–6 MeV/nucleon. The part

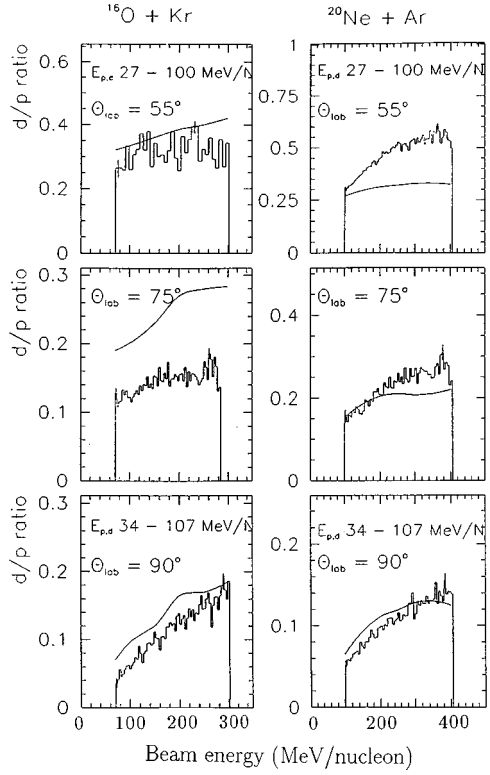

FIG. 4. High energy d/p ratio in O+Kr collisions. The curves represent cascade calculations including coalescence with a cluster radius of 90 MeV/c.

of the available energy that is used for collective expansion is for obvious reasons very small in this case and therefore the emission should follow quite well an evaporative scenario. This is confirmed by the EES calculations that we performed for p+Kr between 150 and 500 MeV but the results are that the d/p ratio for particles with $E>30$ MeV is vastly overestimated whereas the corresponding ratio for $E/A>30$ MeV is rather somewhat underestimated. This shows the difficulties in explaining the high energy deuterons that were selected in the experiment by thermal emission processes.

This conclusion is further confirmed by the calculations with the classical SIMON evaporation code [16]. It shows the same vast overprediction for the $E>30$ MeV ratios but almost no deuterons with energy >30 MeV/nucleon are produced so again the ratio is underpredicted for such very high velocity cutoff. The general conclusion from the comparison to statistical calculations is therefore that nonequilibrium, early emission processes must be introduced to explain the d/p data.

B. Nucleus-nucleus collisions

d/p ratios from heavy ion collisions are presented as histograms in Fig. 4. The lack of data in the O+Kr case below $\sim 70A$ MeV beam energy appears because of problems with the acquisition veto signal for the forward telescopes. For the backward telescopes, data points could be extracted down to beam energies of $\sim 30A$ MeV but there we omit the region $30A-70A$ MeV due to low statistics of deuterons. In the Ne+Ar data the lack of deuteron statistics sets in at $100A$ MeV. The slightly different particle energy/nucleon intervals in forward and backward telescopes appear due to somewhat different detector thicknesses. First we stress that even if the possibilities to compare these data to those from other experiments are limited, they do agree well whenever possible. One example, taken from a comparison to the Ar+Ca data of Jacak *et al.* [18], shows 70° d/p ratios at $92A$ MeV of 0.17 and at $137A$ MeV of 0.25 where our Ne+Ar ratios (75°) are 0.14 and 0.19. When comparing data from the two reactions in Fig. 4, O+Kr and Ne+Ar, one must of course consider the different degree of asymmety. In any participant-spectator prescription the emission systems should have different velocities in the laboratory system and furthermore there may be some different (small) contribution at forward angles from the projectilelike source at the smaller beam energies (see Fig. 2). After considering this, it can be concluded that both reactions show the same smooth increase of the d/p ratio with beam energy and the same decrease of the d/p level with increasing emission angle. We stress, however, again that if the complete yields of particles could be measured, it is likely that the d/p ratio would become less dependent on the beam energy or even turn to a decrease [2,18].

EES calculations must again be given inital source parameters. Only sources near thermal equilibrium with excitation energies <10 MeV/nucleon will decay through evaporation. At high excitation the model provides a monotonically expanding source with cluster formation at very low densities, $\sim 0.1\rho_0$. In view of the three-source picture (see Fig. 2) the dominating source of high energy deuterons and tritons should be the participant with some possible contribution from highly excited target sources. EES calculations for the Ne+Ar case confirm this source selection and indeed also the very wide distribution of excitation energy when looking at inclusive data. Actually complete fusion with full stopping provides ϵ^* from 20 to 90 MeV/nucleon. Once source parameter distributions in ϵ^* and A are chosen for a given beam energy the EES calculations reproduce the experimental d/p and t/d ratios to about the same level as the cascade plus coalescence calculations. Again it is obvious that the high energy composite particles we select in this experiment represent preequilibrium emission which is also confirmed by ''reference'' calculations from the pure evaporative calculations with the SIMON [16] code which can hardly produce any deuterons with $E>27$ MeV/nucleon.

We now turn back to the cascade calculations + coalescence and present in Fig. 4 as curves the d/p ratios calculated with a coalescence radius of $p_0=90$ MeV/c. The general tendency is in agreement with data but there are discrepancies. The angular dependence is not perfect (75° data) in the O+Kr data and the beam energy dependence is weaker than the data for forward emission in the Ne+Ar reaction. Possibly the latter discrepancy can be accounted for by an increasing contribution from the projectilelike source with decreasing beam energy. It is, however, obvious that there is no dramatic difference in p_0, 90 ± 30 MeV/c, between p-nucleus and nucleus-nucleus collisions, and no dramatic change of this parameter with increasing beam energy.

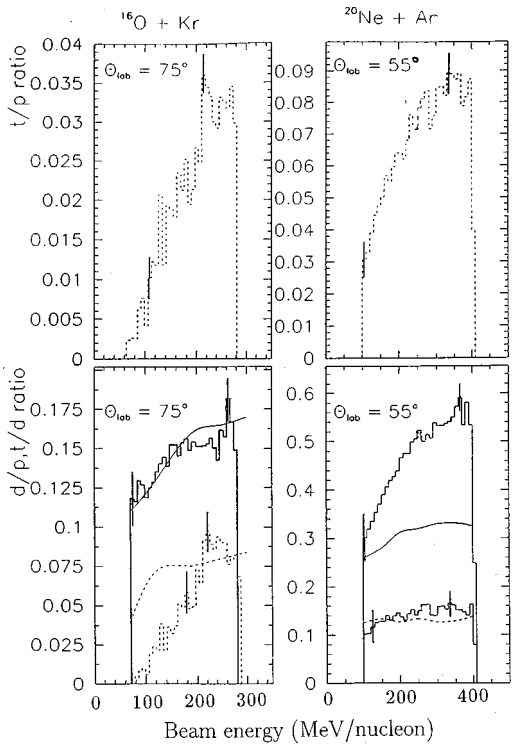

FIG. 5. t/p, d/p, and t/d ratios for particles emitted with energy 27–107 MeV/nucleon at 75° (O+Kr) and at 55° (Ne+Ar). The curves represent the cascade+coalescence calculations with standard values for p_0.

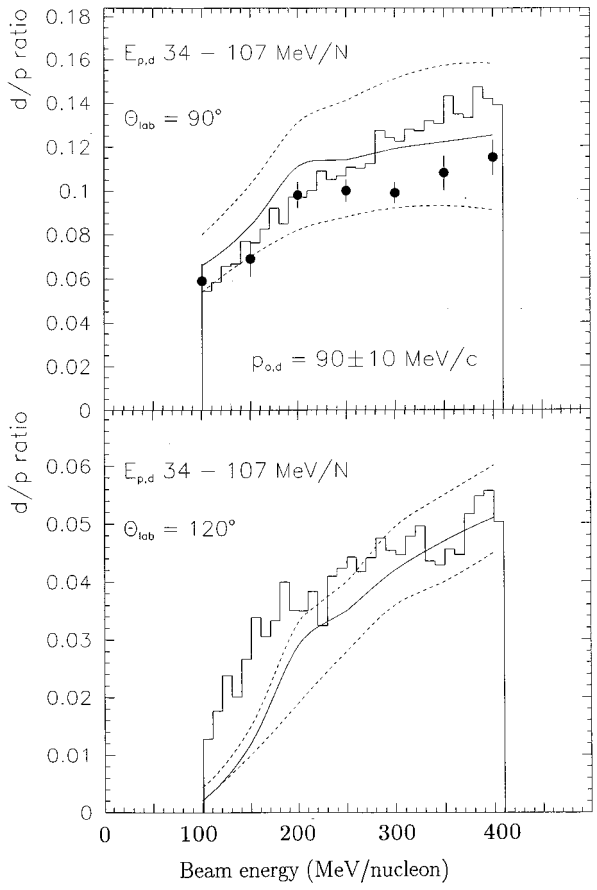

FIG. 6. d/p ratios for particles emitted with energy 34–107 MeV/nucleon at 90° and 120° from Ne+Ar reactions. The curves represent the cascade+coalescence calculations with p_0 = 90 MeV/c (solid line) and 80, 100 MeV/c (dashed line). The points represent NMD+coalescence calculation with p_0 = 90 MeV/c.

Next, t/p ratios are presented in Fig. 5. In the two examples there is again a velocity cutoff introduced, corresponding to an energy/nucleon of 27 MeV/nucleon. This is a very high velocity cutoff for tritons and there is now an even stronger beam energy dependence than for d/p ratios. A comparison between the d/p and t/d ratios is made in the lower figures. The coelescence principle, as prescribed by formula (2), predicts the same ratios if p_0 is taken to be constant. One natural deviation from this may come from the summation over spin if spin coupling is strong,

$$R_{dp}/R_{td}=(2S_d+1)^2/(2S_p+1)(2S_t+1)=9/4. \qquad (3)$$

Actually this factor is very well reproduced in the cascade +coalescence calculations (curves in Fig. 5) and also well reproduced in the O+Kr data, at least for beam energies well above the threshold for high energy composite particle production. The cascade calculations, however, overpredict the t/d ratio for O+Kr by about the same factor as the d/p ratio (see Fig. 4) and in Fig. 5 both calculated curves have been multiplied by 0.6. For the 55°, Ne+Ar ratios the calculations rather underpredicted the d/p ratio (no normalization in Fig. 5) but in this case the t/d ratio comes out in good agreement with data. Possibly, n/p of the emitting system, discussed in Sec. III B, can account for a part of the nonconsistency between d/p and t/d ratios. It should again be noticed that the p_0 radius is 108 MeV/c for tritons, while 90 MeV/c is kept for deuterons following the original tuning [8] from higher energy heavy ion collisions. The general conclusion from all $t/d/p$ ratios is, however, that although the overall agreement between the cascade+coalescence calculations and the data is reasonable, details in angular and beam energy dependences are not reproduced very well. It should again be stressed that with the proper choice of the source ϵ^* and A distributions, the EES calculations predict, e.g., a d/p ratio of 0.3 for the Ne+Ar reaction at 300A MeV and a corresponding t/d ratio of ~0.1, which follow the cascade predictions well. Of course no coalescence is introduced in the EES case.

With respect to selected momentum space and statistics we judge that the backward data in the Ne+Ar reaction contain the best and most clean example of preequilibrium (hot source) emission. These data may be chosen to select among emission mechanisms or to fine-tune the coalescence radius. In Fig. 6 such d/p data are presented (note that the binning is different from Fig. 4) together with (a) the cascade +coalescence calculations with $p_{0,d}$=80, 90, and 100 MeV/c (lower, middle, and upper curves in both figures) and (b) the NMD + coalescence calculations with $p_{0,d}$=90 MeV/c (points in upper figure). From both data and calculations it appears as if there is a change in the d/p-beam energy relation at around 200A MeV pointing to-

wards some change in the emission mechanism. This is most clearly seen in the 120° data where it appears also to be difficult to explain both the low and high beam energy part with the same coalescence radius. Apart from this deviation, it appears as if a coalescence radius of $p_{0,d}=90 \pm 10$ MeV/c well reproduces the emission of fast deuterons. The comparison to NMD + coalescence shows about the same degree of agreement with data as the cascade approach. This reflects of course the fact that both these models can describe singles spectra of protons and neutrons equally well.

V. CONCLUSIONS

Opposite to what is expected for the total yields, we have shown that the high energy (>30 MeV) yields of deuterons and tritons increase smoothly as a function of beam energy both in p-nucleus and nucleus-nucleus collisions. Even if total yields were obtainable, it is doubtful if entropy can be determined from d/p or t/p ratios. No standard statistical model, assuming thermal equilibrium, can reproduce the ratios from our data since the particles appear to be of preequilibrium origin. Microscopic and mean-field+NN are equally successful in reproducing these data. Also the EES model, with proper source distribution input, can account for the nucleus-nucleus collision data to the same degree but is less successful in explaining the p-nucleus data. In the first two kinds of models, inclusion of coalescence as some kind of final-state interaction is necessary. The coalescence radius is surprisingly constant with beam energy and no big differences between p-nucleus and heavy ion collisions are found. Some indications exist that the emission process—or at least the nucleon density—changes in heavy ion collisions at around 200A MeV.

The accelerator staff at the Svedberg Laboratory and the Swedish Research Council for Natural Science are thanked for their support.

[1] S. Nagamiya, M. C. Lemaire, E. Moeller, S. Schnetzer, G. Shapiro, H. Steiner, and I. Tanihata, Phys. Rev. C **24**, 971 (1981).
[2] P. J. Siemens and J. I. Kapusta, Phys. Rev. Lett. **43**, 1486 (1979); J. I. Kapusta and D. Strottman, Phys. Rev. C **23**, 1282 (1981).
[3] I. Mishustin, F. Myhrer, and P. J. Siemens, Phys. Lett. **95B**, 361 (1980).
[4] H. Stöcker, Lawrence Berkeley Laboratory Report No. 12302, 1981.
[5] B. Jacak, H. Stöcker, and G. D. Westfall, Phys. Rev. C **29**, 1744 (1984).
[6] W. Friedman, Phys. Rev. Lett. **60**, 2125 (1988); Phys. Rev. C **40**, 2055 (1989); **42**, 667 (1990).
[7] K. K. Gudima and V. D. Toneev, Sov. J. Nucl. Phys. **27**, 351 (1978).
[8] V. D. Toneev and K. K. Gudima, Nucl. Phys. **A400**, 173c (1983); GSI Report No. GSI-93-52 1993.
[9] G. D. Westfall *et al.*, Phys. Lett. **116B**, 118 (1982).
[10] R. L. Auble *et al.*, Phys. Rev. Lett. **49**, 441 (1982).
[11] C. K. Gelbke, Nucl. Phys. **A400**, 473c (1983).
[12] B. Jakobsson *et al.*, Phys. Rev. Lett. **78**, 3828 (1997).
[13] B. Norén *et al.*, Nucl. Phys. **A489**, 763 (1988).
[14] J. P. Bondorf, D. Idier, and I. Mishustin, Phys. Lett. B **359**, 261 (1995).
[15] W. Weisskopf, Phys. Rev. **52**, 295 (1937).
[16] D. Durand (private communication).
[17] K. K. Gudima, S. G. Mashnik, and V. D. Toneev, Nucl. Phys. **A401**, 329 (1983).
[18] B. Jacak *et al.*, Phys. Rev. C **35**, 1751 (1987).